Wind and Gravity in Shaping Picea Trunks

Markku Larjavaara (markku@pku.edu.cn)
Peking University https://orcid.org/0000-0002-3484-889X
Mikko Auvinen
Ilmatieteen Laitos
Anu Kantola
Luonnonvarakeskus
Annikki Mäkelä
Helsingin Yliopisto

Research

Keywords: Gravity, Norway spruce (Picea abies [L.] Karst.), Sail area, Stem, Thigmomorphogenesis, Trunk taper, Wind drag, Wood

Posted Date: January 7th, 2021

DOI: https://doi.org/10.21203/rs.3.rs-44213/v2

Version of Record: A version of this preprint was published at Trees on May 7th, 2021. See the published version at https://doi.org/10.1007/s00468-021-02138-3.

Wind and gravity in shaping *Picea* trunks

Markku Larjavaara[1]*, Mikko Auvinen[2], Anu Kantola[3], Annikki Mäkelä[4]

[1] Institute of Ecology and Key Laboratory for Earth Surface Processes of the Ministry of Education, College of Urban and Environmental Sciences, Peking University, Beijing 100871, China

[2] Atmospheric Dispersion Modelling, Atmospheric Composition Research, Finnish Meteorological Institute, Finland

[3] Natural Resources Institute Finland (Luke), P.O.Box 2 (Latokartanonkaari 9), FI-00791 Helsinki, Finland

[4] Department of Forest Sciences, P.O.Box 27 (Latokartanonkaari 7), 00014 University of Helsinki, Finland

* Corresponding author (markku@pku.edu.cn)

16 **Abstract**

17 Understanding why trunks (tree stems) are the size that they are is important. However, this
18 understanding is fragmented into isolated schools of thought and has been far from complete.
19 Realistic calculations on minimum trunk diameters needed to resist bending moments caused
20 by wind and gravity would be a significant step forward. However, advancements using this
21 biomechanical approach have been delayed by difficulties in modelling bending of trunks and
22 wind gusts. We felled and measured five Norway spruces (*Picea abies*) in an unthinned
23 monoculture in southeastern Finland planted 67 years earlier. We focused on forces working
24 on storm-bent (maximally bent) trees caused by gravity and the strongest gust in a one-hour
25 simulation with a large-eddy simulation model. The weakest points along the trunks of the
26 three largest trees resisted mean above-canopy wind speeds ranging from 10.2 m s^{-1} to 12.7 m
27 s^{-1} (3.3-fold in the strongest gust), but the two smallest were well protected by a dense layer
28 of leaves from the bending tops of larger trees, and could have resisted stronger winds.
29 Gravity caused approximately one quarter of the critical bending moments. The wind that
30 breaks the trunks in their weakest points is close to breaking them in other points, supporting
31 importance of bending moments caused by wind and gravity in evolution of trunk taper. This
32 approach could also be used to model tree biomasses and how those may change with
33 changing climate.

34

35 **Keywords**

36 Gravity, Norway spruce (*Picea abies* [L.] Karst.), Sail area, Stem, Thigmomorphogenesis,
37 Trunk taper, Wind drag, Wood

38

39

Introduction

Understanding why trees and their trunks (stems) are the size that they are is important for evaluating the potential of forests to mitigate climate change and produce timber. Therefore it is surprising that that the scientific understanding of tree height and diameters along the trunk is fragmented. For example, a question concerning the dimensional determinants of a particular tree trunk may cause surprise and be considered too general by experts in narrow fields, even though understanding trunk dimensions should be considered one of the largest questions in applied ecology.

Research on trunk dimensions can be classified in two ways. Firstly, the classification can be based on the object of the study, i.e. the condition of the forest. Some studies focus on those experiencing natural successions (Anderson-Teixeira et al., 2013), others on tallest old-growth forests (Van Pelt et al., 2016), on plantations subject to self-thinning (Yoda et al., 1963) or silvicultural treatments (Bianchi et al., 2020). Secondly, the classification can be based on whether the approach is descriptive or theoretical. The majority of research on trunk dimensions in forest sciences and research related to forests' role in climate change mitigation is mainly descriptive (e.g. Chave et al., 2014), while much of the physiological and ecological research attempts to explain the causes of the described patterns based on theories. These theories may be grouped based on the function on which the focus is: transport, storage or biomechanical support as explained in the following paragraphs.

Trees passively transport sap (water) up in the sapwood, and the resistance caused by length of the path or need to lift sap against gravity has been used as the basis for modelling maximum tree height (Koch et al., 2004) and growth deceleration in plantations (Ryan and

Yoder, 1997). However, as the heartwood is not contributing to sap transport, diameters along the trunk cannot be understood based on sap transport only, unless heartwood is considered a waste produced e.g. because of ageing (Collalti et al., 2019) or difficulties in using the same sapwood when branches die and grow (Chiba et al., 1988). Phloem transport down the trunk may be similarly limiting tree height due to path length (Woodruff, 2013), but does not explain diameters, unless trunk circumference needs to be increased to increase transport capacity.

Trees are dependent on the storage of water (Scholz et al., 2011) and energy (Schiestl-Aalto et al., 2015) in their woody tissues and this is likely to influence trunk dimensions in certain conditions. For example, baobab (*Adansonia digitata*) trees probably have unusually fat trunks to store water needed to level out seasonal variation in water availability (Chapotin et al., 2006), and lignotubers located at the trunk base can store energy and nutrients enabling rapid sprouting (Canadell and López-Soria, 1998). Trunk dimensions are therefore potentially influenced by storage needs, but this is unlikely to be common and may be restricted to the rare trees that do not form metabolically dead heartwood and therefore cannot increase sapwood volume by adjusting the sapwood-to-heartwood-ratio such as the above-mentioned baobabs (Patrut et al., 2010).

The third general function of trunks in addition to transport and storage, and the only for which heartwood is useful, is to biomechanically support the leaves, branches and trunk sections above the height at which the focus is. Common sense tells that trees exposed to wind or heavy loads need to have thicker trunks for a given height and crown size. These mechanism have been studied experimentally for over two centuries (Telewski, 2016), and the term “thigmomorphogenesis” has become established in the recent decades to describe

90 the responses of plants to mechanical stimuli (Pruyn et al., 2000). Two very different
91 mechanisms may serve as a basis for modelling trunk dimensions biomechanically. Elastic
92 buckling (Euler buckling) can permanently bend trunks if the tree fresh mass and permanent
93 loads, such as epiphytes and lianas, exceed the limit that the trunk can support. Modelling can
94 be performed easily (McMahon, 1973), and normally a “safety factor” is computed
95 describing how far the height of the tree is from a height that leads to buckling. This approach
96 has been used in well-known modelling approaches (e.g. West et al., 1999). However, most
97 trees, with the exception of certain rainforest understorey trees, are far from elastic buckling.
98 For example, Niklas (1994) reported an average safety factor of four. Because of non-
99 linearities, a safety factor of four implies that plants weight is only 1.6% of the weight that
100 would lead to elastic buckling. Furthermore, the safety factor is a misleading concept and
101 should not be interpreted as an indication of biomechanical safety. A safety margin is needed
102 for engineer-designed structures, as they are built and then need to resist variable forces
103 without subsequent adjustments to the structure. However, trees can tune their structure
104 (Bonnesoeur et al., 2016) and a small safety factor is therefore not dangerous, as supporting
105 tissue can be increased according to demand from the increasing height or weight. The wide
106 usage of the theory on elastic buckling shocked Mattheck (2012) and he wrote: “Much to the
107 surprise of the author, failure by buckling has nevertheless been discussed by McMahon
108 (1973), and comparisons have been made between measured height-diameter relations and
109 relations calculated from Euler's buckling theory." The other, more useful, biomechanical
110 approach is based on trunks breaking. Brief buckling e.g. due to a temporary load of snow
111 may not be a problem for the tree if it recovers and is erect most of the time. However, when
112 modelling trunk breakage, even a short period to which the tree has not been able to
113 acclimatize may be fatal. This modelling approach is challenging to follow, as wind speeds
114 are variable in space and time, and trunks, branches and leaves streamline in wind. In both

115 buckling and breaking approaches, diameters needed along the trunk for a given height and
116 other characteristics can be computed based on biomechanics. However, these approaches do
117 not limit height if the diameters are not limited.
118
119 All trees need trunks to transport, to provide biomechanical support and probably also to
120 store, and theories and modelling to understand trunk dimensions should ideally incorporate
121 all of these with appropriate weights. However, in practice realistic modelling of even one of
122 these aspects at a time is challenging. Therefore, it is useful to consider their relative
123 importance. One challenge is that scientists are often experts on only one of these three
124 functions and may therefore overestimate its importance, even though some reviews on all
125 them are available (Badel et al., 2015). Secondly, if building or maintaining a trunk that is
126 superior in any of the three functions causes an energetic cost, all functions would evolve
127 close to the needed level even if the cost improving it relative to the others would be
128 minuscule. An example with an engineer-designed product demonstrates this issue well. An
129 expert focusing on tires may conclude that a given car cannot go faster than e.g. 50 m s^{-1}
130 because of the speed rating of the tires. According to an expert on engines the top speed of
131 the same car is restricted by engine power. Both would be technically correct, but to
132 understand the main reason why markets set the top speed at its level, the challenges in
133 designing, manufacturing, maintaining and operating engines and tires that allow faster
134 speeds must be considered. This reveals that, as improving the speed rating of tires is very
135 easy relative to designing and building a more powerful engine, it makes normally more
136 sense to say that the car does not go faster because the engine is not more powerful and not
137 because of its tires. Similarly, demonstrating that e.g. transporting sap higher than the current
138 height of the tallest trees (Koch et al., 2004) does not necessarily mean that sap transport is
139 the main factor determining maximum heights. Instead, in evolutionary time scales for

example sap transport capacity could improve to a height determined mainly by the biomechanics and energetics of maintaining the living biomass.

We did not properly assess the relative importance of how the functions of trunks influence their dimensions, as that would need to be done by incorporating them into one model. In this paragraph, we just note a few pieces of evidence that indicated to us the direction to take. One approach is to consider the marginal construction and maintenance costs of increasing capacity. Tissue suitable for storage or sap transport may be increased by increasing sapwood to heartwood ratio. Furthermore, sap transport efficiency may be boosted by increasing the density of conduits in angiosperm wood, probably with little or no additional construction costs (Larjavaara, 2021) . However, significant strengthening of the trunk is not possible without substantial additional construction costs, either by increasing diameters or wood density (Larjavaara and Muller-Landau, 2012). Another approach to know about the relative importance of factors influencing trunk dimensions is to compare them in variable environmental conditions that demand for variable transport, storage and biomechanical support needs. This approach underlines the importance of sap transport if height and diameters along the trunk vary according to water availability. The very tallest trees would then be expected to be found in climates and soils with most abundant water, which is not the case, even though the driest climates have a low canopy height (Klein et al., 2015). If storage function was critical in determining trunk dimensions, then seasonality should increase trunk volumes relative to leaf area, which may be the case (Chapotin et al., 2006) but probably only in the case of exceptional species. Finally, with biomechanical support being the most significant, tree heights and forest biomasses should vary depending on winds. This is the case for example with variable distances from the edge and therefore variable wind regimes (Brüchert and Gardiner, 2006). Another perspective on the importance of biomechanics is

165 provided by comparing trees to lianas, which do not have the same biomechanical support
166 needs. Lianas have similar transport and storage needs as trees, and much higher leaf area for
167 a given stem basal area (Ichihashi and Tateno, 2015), which is very likely due to differing
168 biomechanical needs, highlighting their importance to trunk diameters. These considerations
169 led us to explore the role of wind forces and gravity as key determinants of trunk diameters,
170 which is the focus of this article.
171
172 The importance of wind and gravity as a cause of trunk breakage is perhaps what common
173 sense would suggest to be the main factor explaining trunk dimensions. This approach was
174 pioneered in the 19th century (Metzger, 1893) and regularly discussed (Mäkelä, 2002).
175 However, we argue that it still remains underrepresented and that this is probably due to
176 methodological challenges from variable winds. In addition, the streamlining mentioned
177 above and the rarity of the strongest storms that are critical for tree survival and therefore
178 probably drive evolution cause extra challenges. Interesting studies are available on small
179 trees secured on the roof of a moving car (Butler et al., 2012) and medium-sized trees during
180 the leafless period (Niklas and Spatz, 2000), but small (Larjavaara, 2015) and leafless
181 (Mattheck, 2000) trees have different biomechanical constraints than large foliated trees.
182 Large foliated trees have also been examined in impressive studies representing simple
183 (Morgan and Cannell, 1994), more realistic (Spatz and Bruechert, 2000) or excellent detail in
184 tree dimensions (Jackson et al., 2019). However, none of these studies focused on maximally
185 bent trees.
186
187 The objective of this study was to increase our comprehension of determinants concerning
188 tree size and trunk taper, as modified by selective pressures caused by exposure to storm-
189 strength winds, and to examine whether trees are adapted and acclimatized to those. To this

end, we modelled wind in a canopy of a mature storm-bent stand and computed gravity- and wind-caused forces on segments along the trunks based on destructive sampling of *Picea abies* [L.] Karst. trees (Norway spruces). We then focused on the winds that break the trunks at their weakest segment and expected diameters at other segments to be only slightly larger than what was needed to resist the bending moments caused by this wind and gravity.

Methods

Picea abies is a common tree species in its natural range of Northern Europe and Central European mountains and is also planted widely in Central European lowlands and North America (Caudullo et al., 2016). In Finland, *Picea abies* trunk volumes make up 30% of all tree trunk volumes and the volume of harvested trees is 38% of total (Peltola, 2014). It regenerates in intermediate or fertile soils, is the most shade tolerant of the main tree species in Finland and will therefore invade all but the most infertile sandy or peat soils when sufficient time since disturbance has passed (Kuuluvainen and Aakala, 2011). *Picea abies* trees have a straight trunk and long conical crown often reaching the ground. In Finland, the lower branches shed from the lower crown layers in the deep shade of conspecifics. New branches develop annually, forming whorls of branches. Its wood is of low density at 374 kg m^{-3} (Kantola and Makela, 2006) especially when compared to angiosperms (Chave et al., 2009).

We based our study on data collected in 2001 to investigate crown development in three sites around southern Finland in stands after canopy closure (Kantola and Mäkelä, 2004). However, to reduce the complexity of wind gust-related analysis, only a single plot featuring

215 flat terrain is included in this study. The other plots were excluded because of hilly terrain,
216 which alters low-altitude winds in a complex manner (Gardiner et al., 2016). The included
217 plot, described in more detail by Kantola and Mäkelä (2004), was located in Punkaharju at
218 61°49'N, 29°19'E, now part of Savonlinna in southeastern Finland. The local climate is
219 conducive to tree growth, as abundant lakes level out temperature fluctuations during the
220 growing season. The soils in the plot are well above average fertility for the region, classified
221 as *Oxalis*-type (Cajander, 1949), leading to a site index, H_{100} of 32 m. The monoculture of
222 *Picea abies* trees was planted 67 years prior to data collection.
223
224 Three stands with varying thinning histories were studied in the plot but two were excluded
225 from our study because of thinnings, as explained below. The included unthinned stand had a
226 basal area of 44 m^2 ha^{-1} and stand density of 805 ha^{-1}. Five sample trees representing various
227 canopy layers were felled, and their trunks, branches and leaves (i.e. needles) were measured
228 and weighed as described in detail by Kantola and Mäkelä (2004). In summary, trunk
229 diameters were measured below each whorl of branches, and all branches were cut and
230 measured and a subset of them taken to a laboratory for more detailed measurements. The
231 heights and diameters of the five trees at a 1.3-m height ($d_{1.3}$) can be seen in Fig. 8 in the
232 Results section. The percentage of the trunk with living branches of the five sample trees
233 differed between 42–63, being greatest for dominant trees and smallest for trees grown in
234 more suppressed positions. And further, the more suppressed, i.e. thin, trees also had the
235 lightest-weight crowns compared to more dominant ones, which was consistent with the pipe
236 model theory (Kantola and Mäkelä, 2004).
237
238 For this study, we divided the five tree trunks into "segments" and estimated their angle
239 relative to vertical and location relative to the base based on bending and length of all

240 segments below. From the angle relative to vertical we computed their projected area
241 perpendicular to wind direction (i.e. frontal area) and fresh mass based on volumes. We
242 assumed the centre of each segment to be in the whorl of branches and extremes to be located
243 half way between neighbouring whorls. We divided the unmeasured lower branchless trunk
244 into four segments, with the lowest centred at a height of 1.3 m, the remaining three at regular
245 intervals between 1.3 m and the lowest whorl and assumed diameter to simply change
246 linearly, as we anticipated this lowest part of the trunk to contribute only little to the bending
247 moments or to the bending of the trunk.
248
249 The streamlining of trees is complex, and therefore the common approach is to simulate
250 upright trees but with reduced wind drag estimated with a coefficient (Gardiner et al., 2016).
251 We instead focused on the strongest gust and "storm-bent" trees, i.e. trees bent along their
252 trunks as much as they can without breaking (see Fig. 6). This focus was based on the
253 reasoning that even though acclimation is likely to be mainly driven by signals from normal
254 wind speeds (Bonnesoeur et al., 2016), trunks are probably tuned to resist the strongest gusts
255 based on normal winds. Maximum strain in both compression and tension may be assumed to
256 equal the ratio of modulus of rupture and modulus of elasticity. In a bending segment or
257 cylinder, the maximum tension occurs in the outermost fibres of the convex side and
258 maximum compression on the opposite side. However, to simplify the calculations, we
259 assumed rigidity of the segments (as can be seen in Fig. 3) and bending was realised by
260 assuming a change (α) in the deviation of the axis of the segment relative to the segment
261 below:
262

$$\alpha = sin^{-1}\frac{2l\sigma}{dE} \quad (1)$$

263

where l is the length of the segment, σ the modulus of rupture obtained from tree-pulling experiment is 36.26 Mpa (Peltola et al., 2000), d the diameter of the segment at its centre and E the modulus of elasticity is 7730 Mpa (Peltola et al., 2000).

We used the projected area of trunks, branches and leaves (we call their sum "sail area") first for estimating wind speeds and then to compute wind-caused horizontal forces (Online Resource 1).

In addition to the five felled trees, we measured the $d_{1.3}$ of all trees less than seven metres away from the felled ones. We estimated their sail area and its vertical storm-bent distribution by fitting two simple linear regressions to the variables. We then first computed the storm-bent height based on the model in Fig. 1 and then its sail area based on the model in Fig. 2, in which a linear relationship was expected based on biomechanics, as the bending moment is expected to scale roughly with the product of the sail area and the length of the lever (tree height) and the strength of the trunk with the cube of its diameter (Ennos, 2012). We plotted these models for all three stands, but observed the fit to be tight in the unthinned plot only. We surmised that as the previous thinning occurred only 14 years prior to the measurement, the trunk dimensions relative to the sail area (Online Resource 1) were possibly still unbalanced because of too little time since the thinning. We therefore excluded these stands from the analysis.

The mean $d_{1.3}$ of the five felled trees was 0.272 m and they ranged from 0.213 m to 0.328 m, while the surrounding trees around these five had a mean of 0.260 m and a range from 0.167 m to 0.382 m. Because of the tight fit of models in Fig. 1 and Fig. 2, we do not think that extrapolating to some distance out of the range was likely to cause a significant bias.

We wanted to focus on strongest wind gusts that the trees can stand and therefore used turbulence resolving large-eddy simulation (LES) model to describe wind behaviour above and within forest canopies. Because of significant horizontal movement of trees in gusts we had to assume that the forest canopy had a horizontally homogenous sail area and therefore sail area per unit volume (i.e. plant area density) for each 1.5-m thick layer. The large-eddy simulation model PALM (Maronga et al., 2015) was employed to obtain a time-accurate and spatially resolved description of fully developed boundary layer turbulence over continuous forest canopy. The PALM model is specifically tailoured for atmospheric boundary layer turbulence applications and has been optimized for massively parallel supercomputing environments. The model implements the conservation equations governing atmospheric boundary layer turbulence employing finite-difference discretization on a staggered Cartesian grid. The system of equations is solved using a third-order accurate Runge-Kutta time-stepping scheme and fifth-order accurate upwind biased spatial discretization scheme (Wicker and Skamarock, 2002). The forest canopy is modelled assuming a porous homogenous medium within each 1.5-m layer, whose porosity varies according to the measured vertical sample-averaged plant area density distribution of the trees.

A vast majority of the drag caused by the forest canopy was assumed to be pressure drag, and therefore the drag force (f) is implemented in PALM as:

$$\vec{f} = C_d P |\vec{u}| \vec{u}, \quad (2)$$

where C_d is the drag coefficient for forest canopy, P is the vertical plant area density profile of the forest, and $\vec{u}$ is the spatially and temporally resolved wind velocity vector whose

magnitude is denoted as $|\vec{u}|$. We set C_d at 0.2 as suggested by Katul (1998). The wind simulations were performed on a rectangular domain with *Lx* of 3.84 km, *Ly* of 1.28 km and *Lz* of 0.52 km as streamwise, lateral and vertical dimensions, respectively. Wind was driven with a prescribed pressure gradient at z > 250 m, allowing the lower-altitude flow to attain a constant momentum flux layer, which is characteristic for atmospheric boundary layer flows (Stull, 2012). The magnitude of the pressure gradient was set sufficiently high to achieve very high Reynolds number conditions, which ensures that the associated turbulence solution attains a state that is independent of wind speed. That is, if the wind speed were further increased, the turbulent structures and dynamics would remain statistically identical. This Reynolds number independence allows one representative turbulent wind solution to be freely scaled (especially upward) to represent other wind conditions. The simulation for the (scalable) reference wind was initially run for one hour to allow the flow to reach a statistically stationary state. The simulation was then continued for an additional hour during which detailed wind velocity time series is collected every 3 s (at 1/3 Hz) across the entire depth of the forest canopy from a 0.5-km^2 monitoring plane with 409 x 205 locations. This time series contains a sample of 105.6 x 10^6 instantaneous wind events impacting the forest canopy. As the main interest is on gusts whose duration is sufficient to cause further displacements in the tree trunks, two consecutive wind events are averaged to yield a conservative approximation for a 3-s gust. Thus, the time series contained approximately 50 x 10^6 gust events, which is considered a sufficiently large sample size to capture rare gust events that impose the largest risk for trunk failure. The gust events causing the maximal bending moments were searched by considering the forest canopy to contain trees with uniform horizontal cross-sections (just for the sake of wind gust analysis). The bending moment for each model tree was computed for all 3-s gust events and the maximum events (time and location) were stored. The wind speed profile spanning across the tree height was

then obtained from this location and instance. The selected gust event provided the most realistic estimation for the critical velocity distribution during a probable failure event.

In addition to the normal simulation named "Dense", we performed a second simulation with half of the sail area removed from all heights above ground (i.e. "Thinned") and a third simulation with trunks and branches remaining but leaves removed (i.e. "Leafless"). However, it is important to note that these two secondary simulations violate the basis of our modelling of trees evolved to withstand a given above-canopy wind speed by equal strain along the trunk, as a sudden thinning or defoliation would disturb the balance to which trees have acclimated and trunks would therefore likely break from a severely underbuilt segment before full bending is reached.

We computed the bending moments by adding moments from all segments and associated branches and leaves above the segment in question (Fig. 3). We obtained the weights, i.e. the vertical forces, by adding water contents of 0.79 for the trunk, 1.41 for the branches and 2.24 for leaves (Kantola and Makela, 2006; Kärkkäinen, 1985) to the dry masses (Kantola and Mäkelä, 2004) and multiplying by the gravity constant (9.82 m s^{-2}). We did not take physical contact between the trees into account.

The critical bending moment, i.e. the maximum bending moment that a cylindrical segment can resist (m_r) is:

$$m_r = \frac{\sigma \pi d^3}{32} \quad (3)$$

where σ is modulus of rupture and d is the diameter of the segment (Ennos, 2012). The sum of gravity- and wind-caused bending moments that cause this same m_r for the trunk segment is:

$$m_r = r^2 \sum m_u + \sum m_g, \quad (4)$$

where $\sum m_g$ is the sum of all gravity-caused bending moments of all the segments and associated branches and leaves above, $\sum m_u$ is the sum of all wind-caused bending moments from segments and associated branches and leaves above in a reference above-canopy mean wind speed and r is the ratio of the maximum and reference (to compute $\sum m_u$) mean above-canopy wind speeds based on the wind profile obtained from the PALM model. These steps are shown as a flow chart in Fig. 4.

We then computed critical wind speeds that break the trunks in their weakest segments and compared diameters of other segments to those needed to resist this wind. We did not "tune" the approach or parameters to obtain a desirable fit. Below, we report the results from the analysis planned before beginning analysing the data with the exception of exclusion of recently thinned plots.

Results

Most of the sail area of the five felled trees is caused by leaves and is located, once the trees are storm-bent, at a height of 15–21 m (Fig 5a). When the surrounding trees are added, the layer of dense sail area thickens, mainly upward (Fig 5b), but is still surprisingly thin for a tree species having an unusually long crown. The lack of thinnings in the studied stand has

385 probably resulted in unusually small crown ratios and thin trunks enabling considerable
386 bending, both of which thin the layer of dense sail area in a storm-bent stand.
387
388 The gust wind speeds are weak below 8 m, and increase roughly linearly upwards through the
389 main sail area in Dense and Thinned stands (Fig. 5c). However gust wind is significant down
390 to the ground in the Leafless stand (Fig. 5c).
391
392 The weight of the branchless lower parts of the trunks of all five felled trees is important, but
393 they cause bending moments only to the lower segments of the trunk. These moments are
394 small, as the segments are nearly vertically aligned (Fig. 6). The weights from the upper
395 segments and associated branches and leaves that produce potentially more significant
396 bending moments are roughly evenly divided by those caused by the trunk, branches and
397 leaves (Fig. 6). The comparison between trees illustrates how trees with larger $d_{1.3}$ (Tree4 and
398 Tree5) have correspondingly heavier crowns but the differences are small. The differences
399 between the five trees are much more significant when the horizontal vectors caused by wind
400 are examined (Fig. 6). The smallest trees experience much greater forces caused by gravity
401 than wind, whereas both forces are of the same magnitude in the crowns of the largest trees.
402 However, the wind-caused forces act higher up along the trunk and their direction also causes
403 greater strengthening requirements for the lower trunk. Because the top of storm-bent Tree1
404 is only at a height of 16.1 m, it is well protected by more rigid taller trees (Fig. 6).
405 Interestingly, because the shorter trees bend more, the horizontal displacement caused by
406 wind is approximately the same for all five trees, ranging from 12.7 m (Tree5) to 14.3
407 (Tree3).
408

409 Gravity from all segments and associated branches and leaves above the height at which the
410 focus is 18–27% of the bending moment that breaks a tree at a height of 1.3 m (Fig. 7). This
411 proportion increases upwards to a height of 12–15 m with the lowest branches and then
412 decreases down to a rounded 0% for the tops of the trees. However, as bark is included in the
413 used *d* and the wood characteristics are unusual for the topmost segments, the estimated
414 proportion is likely to be a severe underestimation. Nevertheless, the proportion of gravity
415 relative to the critical bending moment clearly decreases upwards in the canopy.
416
417 Fig. 8 demonstrates the dimensions of the five felled trees without wind and in addition to the
418 measured diameters, the diameters needed to resist an above-canopy mean wind of 10.2 m s^{-1},
419 which is the speed that is at the limit of breaking Tree4. This can be seen from the dotted red
420 line contacting the solid black line at a height of 13.9 m. Tree3 and Tree5 are able to resist
421 similar mean above-canopy wind speeds (12.7 m s^{-1} and 11.3 m s^{-1}), and therefore the
422 modelled taper is similar to the measured taper (Fig. 8). However, for Tree2 and especially
423 Tree1, a significantly thinner trunk would be sufficient to withstand the simulated gust with
424 an above-canopy mean wind of 10.2 m s^{-1}. The simulated gust increases wind speeds
425 considerably, reaching 34.2 m s^{-1} above-canopy (height of 29.25 m) and decreasing
426 downwards as shown in Fig. 5c, with a speed of 25.9 m s^{-1} in the upper part (height of 21.75
427 m) of the storm-bent main canopy and 5.6 m s^{-1} in the lower part (height of 12.75 m).
428
429 The above-canopy mean wind speed in the thinned stand is surprisingly similar to that above
430 the dense stand, and rounds to the same 10.2 m s^{-1} in the equivalent meteorological situation
431 and is slightly weaker in the strongest gust at 33.2 m s^{-1}. However, the winds are stronger
432 within the canopy, and for all except Tree1, greater diameters would have been needed to
433 resist breaking (Fig. 8), indicating that thinnings increase the risk of stem breakage.

The wind simulation for a leafless stand resulted in an above-canopy mean wind speed of 14.6 m s^{-1} (gust 36.3 m s^{-1}) in the same meteorological situation as discussed above and the wind penetrated the stand with much more force (Fig. 5c). A significantly smaller diameter for all trees and along all heights would be sufficient in this situation (Fig. 8), as sail areas of the trees decreased.

Discussion

We developed a novel approach to model bending moments of storm-bent trees caused by wind and gravity and applied this to an unthinned middle-aged *Picea* stand originated from planted seedlings. We focused on winds that break the weakest segments and observed a close match of modelled and the actual diameters along other segments their trunks for most of the trees (Fig. 8). Therefore, we may conclude that these bending moments are probably important in determining trunk diameter and shape, but we are unable to compare importance of alternative determinants of tree size such as sap transport. The relatively small contribution of a tree's own mass (Fig. 7) indicates that, if to simplify only gravity or wind can be included in the modelling, wind would probably be a better choice, even in a dense unthinned stand (e.g. Larjavaara, 2010) with small sail areas relative to fresh masses. The studied trees where probably much closer to elastic buckling than plants in the dataset of Niklas (1994) and may be close to bending due to the extra weight of snow.

Our simulated winds may be compared to those within (at a height of 9 m) and above (at a height of 23 m) a 16-m tall *Pinus sylvestris* stand during a summer microburst that toppled

459 over trees approximately 300 m from the wind measurements (Järvi et al., 2007). The
460 microburst caused one-minute mean wind speeds of ca. 14 m s^{-1} above and 5 m s^{-1} within the
461 canopy. The above-canopy speed is close to the winds that our five trees can resist, with the
462 exception of Tree1 (Fig. 8). Furthermore, the wind speed within the relatively sparse *Pinus*
463 canopy corresponds to values that may have been expected based on our wind profiles (Fig.
464 5c). However, the variation in windspeed measured by Järvi et al. (2007) was much lower, as
465 their "instantaneous" above-canopy wind speeds peaked at only just above 20 m s^{-1}. This may
466 indicate that our biomechanical computations overestimated the resistance of trees to bending
467 forces. However, as the damaged *Pinus* trees were located some distance away from the
468 anemometers, it is likely they experienced much stronger wind speeds than recorded at the
469 specific location of the sensors.
470
471 Our objectives were to understand more about trunk taper based on wind and the risks that
472 trees potentially take, whereas the majority of research linking taper, wind and risks inversely
473 attempt to estimate risks from taper and winds (Gardiner et al., 2008). The demand for advice
474 from forest managers is substantial both in plantations (Gardiner et al., 2016) and urban
475 setting (Sæbø et al., 2003), and advances have been impressive (Gardiner et al., 2019).
476 However, a pessimist may argue that scientists will never be "wiser" than an acclimated tree
477 in understanding the local wind profile and risks caused by extreme gusts. From an
478 evolutionary perspective, trees balance between having their trunks breaking in a storm and
479 overinvesting in trunk tissue and being overtopped by their neighbours growing faster. A
480 winning strategy optimally balancing between the deadly "ditches" on both sides depends on
481 the position of the other ditch. Hence, in a situation with fierce competition and high
482 likelihood of being overtopped by neighbours, such as in middle-aged dense plantations, the
483 risk on trunk breakage in a storm is increased. Therefore, the most fruitful theoretical (not

484 just statistical and descriptive) way to estimate the risk of trunk breakage may be based on
485 competition for height from an evolutionary perspective. Physical modelling, such as that
486 used in this article but inversely, is more promising for trees in situations have not acclimated
487 to, e.g. after their neighbours have been harvested (e.g. Peltola et al., 1999).
488
489 In our simulation of the strongest gust, it is remarkable how a *Picea abies* monoculture,
490 characterised by long, conical, and slender crowns, forms a relatively thin layer of dense sail
491 area of sail area at approximately 18 m above ground during a gust. To support a larger leaf
492 mass, a tree needs to build a thicker trunk to resist the wind drag and gravity acting on this
493 additional mass. Even without additional height when unbent, the additional diameter reduces
494 bending and the storm-bent height increases. Because trees with thicker trunks are normally
495 also taller, they have greater wind drag caused by bending moments because of greater sail
496 area and this area being located in greater winds because of greater unbent height but also
497 reduced bending. The thicker trees in a stand are responsible for blocking wind and
498 protecting the smaller "biomechanical free-riders". This mechanism operates as a balancing
499 force, i.e. negative feedback, in stand development, thanks to which height growth of shorter
500 trees is boosted.
501
502 Tree1 is much thicker and Tree2 is to some extent thicker than they need to be to resist the
503 modelled gust. Their positions in the canopy may have weakened rapidly, leaving their
504 thicker trunks as a legacy of a time when they needed strength for a larger leaf area, but
505 biomechanically they would not then need new diameter growth. Also the transport-focused
506 perspective offers an alternative explanation. When trees become suppressed in the canopy,
507 they rapidly lose their lower branches and their crown length grows more slowly than their
508 height, reducing their crown ratio. This change in growth pattern may be regarded as an

509 evolutionary response to competition for light (e.g. Mäkelä, 1985). In this process, active
510 wood, i.e. sapwood, related to the receding branches loses its connection to the foliage and
511 gradually turns into inactive heartwood. Empirical evidence and eco-evolutionary balance
512 theories suggest that active wood area and foliage area are in balance with each other (Chiba
513 et al., 1988; Mäkelä and Valentine, 2006; Shinozaki et al., 1964). Losing the active wood
514 related to the receding branches therefore creates a need for new diameter growth to build
515 new sapwood, as the existing inactive wood can no longer be used for water transport. If we
516 assume that all these selective pressures, related to biomechanics, water transport, and
517 competition for light, are present in the tree population, then our results suggest that
518 biomechanics dominate trunk dimensions of dominant trees (see also Mäkelä and Valentine,
519 2006), while with suppressed trees the balance has possibly shifted from biomechanics
520 towards sap transport. Another reason for our result that smaller trees have larger diameters
521 than apparently necessary may be that our wind model severely overestimates the steepness
522 of the vertical wind profile. It is also possible that supressed trees occasionally experience
523 unusually strong gusts that penetrate the canopy but which was not our "strongest gust" due
524 to our sampling, and are therefore seemingly overbuilt. If suppressed trees are
525 biomechanically overbuilt because of sap transport, they would be expected to survive storms
526 more likely than dominants, but if they are not biomechanically overbuilt, due to problems in
527 our wind modelling, they are likely on the contrary be more vulnerable due to greater risk-
528 taking. However, survival of suppressed trees could also be due to their strategy to benefit
529 from the failure of their supressors.
530
531 The tops of all five trees appear overbuilt. We can try to understand this by comparing small
532 trees of the same height that may initially seem to have nearly identical biomechanical
533 constraints. Coincidentally, both small *Picea* trees and residue treetops have commonly been

used as Christmas trees in Finland and are easy to differentiate even from a distance. Treetops need to resist much stronger winds but can streamline easier, as their bases are tilted thanks to the bending lower trunk. Probably most importantly, treetops cannot rely on the "shrub strategy" of bending all the way to the ground to remain unharmed (Larjavaara, 2015). This makes small trees resistant to the strongest winds and heaviest snowloads, as they can bounce back after a gust has passed or the snow has melted. Treetops however, cannot rely on ground support during gusts, but this is probably not a problem for the well-streamlined tops of *Picea abies* (Fig. 6). Snow weight, which may be significant in the region, is a possible reason for the seemingly overbuilt tops in our dataset (Peltola et al., 1999), especially when temperatures are close to freezing or when direct condensation occurs on trees.

We focused on an unthinned boreal monoculture, i.e. nearly the simplest stand imaginable – only treetops could potentially have been easier to understand in an ice-free climate. We nevertheless had to make many simplifying assumptions. The risk of resonating with the wind is a serious concern in designing structures, such as bridges, and the risk of trees swaying with a pulsing wind has often been the focus of trunk breakage literature (Niklas and Spatz, 2012). However, air flow modelling does not seem to create such winds (Gardiner et al., 2019) and is rarely seen in dozens of videos found on the Internet that depict uprooting or trunk breakage (ML personal observation). Similarly, torsional forces have attracted some attention (Skatter and Kucera, 2000), but it is likely that strengthening the trunks to resist twisting could be achieved by adjusting wood characteristics without increasing trunk diameters. Uprooting possibly being more common than trunk breakage is one argument against the biomechanical modelling of trunks, but this does not rule out the importance of trunk dimensions on trunk failure. In their evolutionary history, trees have probably balanced the risks of uprooting and trunk breakage depending on the level and variability of risks and

559 on the cost of strengthening them. Our assumptions that the same level of streamlining occurs
560 at all heights (Online Resource 1) and invariable, modulus of rupture (σ) and modulus of
561 elasticity (E), may be far from realistic but probably do not interfere significantly with our
562 comparison between trees and along the trunk of one tree, except perhaps in the tops which
563 may in reality be more flexible due to juvenile wood and therefore e.g. the relative
564 importance of gravity would be underestimated (Fig. 7). Choosing the value for drag
565 coefficient (C_d) was rather arbitrary as always. Furthermore, we did not attempt to include
566 physical contact with neighbours influencing the bending forces. Such canopy contacts may
567 be harmful, as tree tissue may be damaged, but on the other hand they may save a tree that is
568 supported by a neighbour in extreme winds.
569
570 Our greatest concern relates to dealing with streamlining and the homogeneousness of the sail
571 area. We assumed 50% streamlining for branches and none for leaves (Online Resource 1).
572 This is probably an underestimation (Peltola et al., 1999), but perhaps surprisingly it does not
573 strongly influence this kind of analysis related to trunk diameters, as despite streamlining
574 reducing wind drag caused by a given wind speed, it increases wind speeds within the stand.
575 For example, the Thinned simulation with half of the sail area removed corresponds to the
576 Dense simulation with streamlining reducing the projected area to half its original size. This
577 allows us to estimate the sensitivity of our results to assumptions on streamlining.
578 Interestingly, the wind-caused bending moments were larger for two of our five trees, with
579 50 % stronger streamlining, while they were smaller for three trees. This indicates that our
580 results are not very sensitive to streamlining, as the increasing wind speed due to streamlining
581 compensates for the reduced sail area. Similarly, the spatial grouping of sail area is probably
582 important and drastically influences both winds and the drags that they cause. However,
583 again it is possible that reduced winds for a given wind speed cause greater within-canopy

584 winds thanks to the clustering of sail area, and their impacts may roughly even out as with the
585 cause of streamlining.
586
587 Our approach could be utilized in several applications. Evolutionary simulations could
588 optimize trunk dimensions by considering the benefits of being a biomechanical free-rider
589 and relying on larger neighbour trees to withstand wind, but potentially face local extinction
590 if all canopy species or individuals take excessive risks and rely on trunks of others not
591 breaking. Other mechanistic modelling approaches (Kalliokoski et al., 2016), which are
592 potentially especially valuable when optimizing forest management in changed conditions,
593 may also benefit from incorporation of wind- and gravity-driven trunk diameter modelling,
594 e.g. by increasing detail in the direction pointed by Eloy et al. (2017).
595
596 **Availability of data and materials**
597 The dataset will be made available in a location specified later.
598
599 **Conflict of interest**
600 The authors declare that they have no conflict of interest
601
602 **Funding**
603 ML acknowledges Peking University for funding.
604
605 **Author's contributions**
606 ML and AM developed the research idea, AK designed and implemented the data collection
607 procedure supervised by AM, MA performed the wind simulations and wrote the first draft of
608 its description, ML performed the other analyses, prepared the figures and wrote the first

draft of the other sections, and all authors participated in producing the final version of the manuscript.

Acknowledgements

We thank Tapio Linkosalo for discussions in the early stages of the research process and Stella Thompson for English language editing.

615 # References

616

617 Anderson-Teixeira KJ, Miller AD, Mohan JE, Hudiburg TW, Duval BD, DeLucia EH (2013) Altered
618 dynamics of forest recovery under a changing climate. Global Change Biology 19: 2001-2021
619 Badel E, Ewers FW, Cochard H, Telewski FWJFiPS (2015) Acclimation of mechanical and hydraulic
620 functions in trees: impact of the thigmomorphogenetic process 6: 266
621 Bianchi S, Huuskonen S, Siipilehto J, Hynynen J (2020) Differences in tree growth of Norway spruce
622 under rotation forestry and continuous cover forestry. Forest Ecology and Management 458
623 Bonnesoeur V, Constant T, Moulia B, Fournier M (2016) Forest trees filter chronic wind-signals to
624 acclimate to high winds. New Phytol. 210: 850-860
625 Brüchert F, Gardiner B (2006) The effect of wind exposure on the tree aerial architecture and
626 biomechanics of Sitka spruce (Picea sitchensis, Pinaceae). American journal of botany 93: 1512-1521
627 Butler DW, Gleason SM, Davidson I, Onoda Y, Westoby M (2012) Safety and streamlining of woody
628 shoots in wind: an empirical study across 39 species in tropical Australia. New Phytol. 193: 137-149
629 Cajander AK (1949) Forest types and their significance. Acta Forestalia Fennica 56: 1-72
630 Canadell J, López-Soria L (1998) Lignotuber reserves support regrowth following clipping of two
631 Mediterranean shrubs. Functional Ecology 12: 31-38
632 Caudullo G, Tinner W, de Rigo D (2016) Picea abies in Europe: distribution, habitat, usage and
633 threats. In: San-Miguel-Ayanz J, de Rigo D, Caudullo G, Houston Durrant T, Mauri A (eds) European
634 Atlas of Forest Tree Species
635 Chapotin SM, Razanameharizaka JH, Holbrook NM (2006) Baobab trees (Adansonia) in Madagascar
636 use stored water to flush new leaves but not to support stomatal opening before the rainy season.
637 New Phytol. 169: 549-559
638 Chave J, Coomes D, Jansen S, Lewis SL, Swenson NG, Zanne AE (2009) Towards a worldwide wood
639 economics spectrum. Ecology Letters 12: 351-366
640 Chave J, Rejou-Mechain M, Burquez A, Chidumayo E, Colgan MS, Delitti WBC, Duque A, Eid T,
641 Fearnside PM, Goodman RC, Henry M, Martinez-Yrizar A, Mugasha WA, Muller-Landau HC,
642 Mencuccini M, Nelson BW, Ngomanda A, Nogueira EM, Ortiz-Malavassi E, Pelissier R, Ploton P, Ryan
643 CM, Saldarriaga JG, Vieilledent G (2014) Improved allometric models to estimate the aboveground
644 biomass of tropical trees. Global Change Biology 20: 3177-3190
645 Chiba Y, Fujimori T, Kiyono Y (1988) Another interpretation of the profile diagram and its availability
646 with consideration of the growth process of forest trees. Journal of the Japanese Forestry Society 70:
647 245-254
648 Collalti A, Tjoelker MG, Hoch G, Mäkelä A, Guidolotti G, Heskel M, Petit G, Ryan MG, Battipaglia G,
649 Matteucci G (2019) Plant respiration: controlled by photosynthesis or biomass? Global Change
650 Biology
651 Eloy C, Fournier M, Lacointe A, Moulia B (2017) Wind loads and competition for light sculpt trees
652 into self-similar structures. Nat. Commun. 8: 1014
653 Ennos AR (2012) Solid biomechanics. Princeton University Press
654 Gardiner B, Achim A, Nicoll B, Ruel J-C (2019) Understanding the interactions between wind and
655 trees: an introduction to the IUFRO 8th Wind and Trees Conference (2017). Forestry: An
656 International Journal of Forest Research 92: 375-380
657 Gardiner B, Berry P, Moulia B (2016) Wind impacts on plant growth, mechanics and damage. Plant
658 Science 245: 94-118
659 Gardiner B, Byrne K, Hale S, Kamimura K, Mitchell SJ, Peltola H, Ruel J-C (2008) A review of
660 mechanistic modelling of wind damage risk to forests. Forestry: An International Journal of Forest
661 Research 81: 447-463
662 Ichihashi R, Tateno M (2015) Biomass allocation and long-term growth patterns of temperate lianas
663 in comparison with trees. New Phytol. 207: 604-612

Jackson T, Shenkin A, Wellpott A, Calders K, Origo N, Disney M, Burt A, Raumonen P, Gardiner B, Herold M (2019) Finite element analysis of trees in the wind based on terrestrial laser scanning data. Agricultural forest meteorology 265: 137-144
Järvi L, Punkka A-J, Schultz DM, Petäjä T, Hohti H, Rinne J, Pohja T, Kulmala M, Hari P, Vesala T (2007) Micrometeorological observations of a microburst in southern Finland. Atmospheric Boundary Layers. Springer, pp 187-203
Kalliokoski T, Mäkinen H, Linkosalo T, Mäkelä A (2016) Evaluation of stand-level hybrid PipeQual model with permanent sample plot data of Norway spruce. Canadian Journal of Forest Research 47: 234-245
Kantola A, Makela A (2006) Development of biomass proportions in Norway spruce (Picea abies L. Karst.). Trees-Structure and Function 20: 111-121
Kantola A, Mäkelä A (2004) Crown development in Norway spruce [Picea abies (L.) Karst.]. Trees Structure & Functioning 18: 408-421
Kärkkäinen M (1985) Puutiede. Sallisen kustannus
Katul G (1998) An investigation of higher-order closure models for a forested canopy. Boundary-Layer Meteorology 89: 47-74
Klein T, Randin C, Korner C (2015) Water availability predicts forest canopy height at the globalscale. Ecology Letters 18: 1311-1320
Koch GW, Sillett SC, Jennings GM, Davis SD (2004) The limits to tree height. Nature 428: 851-854
Kuuluvainen T, Aakala T (2011) Natural forest dynamics in boreal Fennoscandia: a review and classification. Silva Fennica 45: 823-841
Larjavaara M (2010) Maintenance cost, toppling risk and size of trees in a self-thinning stand. Journal of Theoretical Biology 265: 63-67
Larjavaara M (2015) Trees and shrubs differ biomechanically. Trends Ecol. Evol. 30: 499-500
Larjavaara M (2021) What would a tree say about its size? Frontiers in Ecology and Evolution 8
Larjavaara M, Muller-Landau HC (2012) Still rethinking the value of high wood density. American Journal of Botany 99: 165-168
Mäkelä A (1985) Differential games in evolutionary theory: height growth strategies of trees. Theoretical Population Biology 27: 239-267
Mäkelä A (2002) Derivation of stem taper from the pipe theory in a carbon balance framework. Tree Physiology 22: 891-905
Mäkelä A, Valentine HT (2006) Crown ratio influences allometric scaling in trees. Ecology Letters 87: 2967-2972
Maronga B, Gryschka M, Heinze R, Hoffmann F, Kanani-Sühring F, Keck M, Ketelsen K, Letzel MO, Sühring M, Raasch S (2015) The Parallelized Large-Eddy Simulation Model (PALM) version 4.0 for atmospheric and oceanic flows: model formulation, recent developments, and future perspectives. Geoscientific Model Development Discussions 8
Mattheck C (2000) Comments on" Wind-induced stresses in cherry trees: evidence against the hypothesis of constant stress levels" by KJ Niklas, H.-C. Spatz, Trees (2000) 14: 230-237. Trees Structure & Functioning 15
Mattheck GC (2012) Trees: the mechanical design. Springer Science & Business Media
McMahon T (1973) Size and shape in biology. Science 179: 1201-1204
Metzger K (1893) Der Wind als maßgebender Faktor für das Wachsthum der Bäume. Mündener Forstliche Hefte 5: 35-86
Morgan J, Cannell MG (1994) Shape of tree stems—a re-examination of the uniform stress hypothesis. Tree physiology 14: 49-62
Niklas KJ (1994) INTERSPECIFIC ALLOMETRIES OF CRITICAL BUCKLING HEIGHT AND ACTUAL PLANT HEIGHT. American Journal of Botany 81: 1275-1279
Niklas KJ, Spatz H-C (2000) Wind-induced stresses in cherry trees: evidence against the hypothesis of constant stress levels. Trees Structure & Functioning 14: 230-237
Niklas KJ, Spatz HC (2012) Plant Physics. University of Chicago Press

Patrut A, Mayne DH, von Reden KF, Lowy DA, Van Pelt R, McNichol AP, Roberts ML, Margineanu D (2010) Fire history of a giant African baobab evinced by radiocarbon dating. Radiocarbon 52: 717-726

Peltola A (2014) Metsätilastollinen vuosikirja 2014

Peltola H, Kellomaki S, Hassinen A, Granander M (2000) Mechanical stability of Scots pine, Norway spruce and birch: an analysis of tree-pulling experiments in Finland. Forest Ecology And Management 135: 143-153

Peltola H, Kellomäki S, Väisänen H, Ikonen V-P (1999) A mechanistic model for assessing the risk of wind and snow damage to single trees and stands of Scots pine, Norway spruce, and birch. Canadian Journal of Forest Research 29: 647-661

Pruyn ML, Ewers III BJ, Telewski FWJTP (2000) Thigmomorphogenesis: changes in the morphology and mechanical properties of two Populus hybrids in response to mechanical perturbation 20: 535-540

Ryan MG, Yoder BJ (1997) Hydraulic limits to tree height and tree growth. Bioscience 47: 235-242

Sæbø A, Benedikz T, Randrup TBJUF, Greening U (2003) Selection of trees for urban forestry in the Nordic countries 2: 101-114

Schiestl‐Aalto P, Kulmala L, Mäkinen H, Nikinmaa E, Mäkelä A (2015) CASSIA–a dynamic model for predicting intra‐annual sink demand and interannual growth variation in S cots pine. New Phytol. 206: 647-659

Scholz FG, Phillips NG, Bucci SJ, Meinzer FC, Goldstein G (2011) Hydraulic capacitance: biophysics and functional significance of internal water sources in relation to tree size. Size-and age-related changes in tree structure and function. Springer, pp 341-361

Shinozaki K, Yoda K, Hozumi K, Kira T (1964) A quantitative analysis on plant form - The pipe model theory. I - Basic analyses. Japanese Journal of Ecology 14: 97-105

Skatter S, Kucera B (2000) Tree breakage from torsional wind loading due to crown asymmetry. Forest Ecology Management 135: 97-103

Spatz H-C, Bruechert F (2000) Basic biomechanics of self-supporting plants: wind loads and gravitational loads on a Norway spruce tree. Forest Ecology Management 135: 33-44

Stull RB (2012) An introduction to boundary layer meteorology. Springer Science & Business Media

Telewski FW (2016) Flexure wood: mechanical stress induced secondary xylem formation. Secondary Xylem Biology. Elsevier, pp 73-91

Van Pelt R, Sillett SC, Kruse WA, Freund JA, Kramer RD (2016) Emergent crowns and light-use complementarity lead to global maximum biomass and leaf area in Sequoia sempervirens forests. Forest Ecology Management 375: 279-308

West GB, Brown JH, Enquist BJ (1999) A general model for the structure and allometry of plant vascular systems. Nature 400: 664-667

Wicker LJ, Skamarock WC (2002) Time-splitting methods for elastic models using forward time schemes. Monthly weather review 130: 2088-2097

Woodruff DR (2013) The impacts of water stress on phloem transport in Douglas-fir trees. Tree physiology 34: 5-14

Yoda K, Kira T, Ogawa H, Hozumi K (1963) Self-thinning in overcrowded pure stands under cultivated and natural conditions. Journal of Biology, Osaka City University 14: 107-129

760 **Figure captions**

761

762 Figure 1. Storm-bent height of the five felled trees plotted against $d_{1.3}$ and a fitted linear

763 regression model. R^2 is the coefficient of determination.

764

765 Figure 2. Storm-bent height of the five felled trees multiplied by their sail area (projected

766 area of trunk, branches and leaves) plotted against the cube of $d_{1.3}$ and a fitter linear

767 regression model. R^2 is the coefficient of determination.

768

769 Figure 3. An example of how we computed the bending moments from the forces caused by

770 gravity and wind blowing from left to right. The “dashed” line represents storm-bent Tree3

771 with 18 uneven segments visible out of its 35 segments. The vectors show how we

772 computed the moment caused by the 11th topmost segment to the 3rd lowest segment

773 (both of which are highlighted with a thicker red line).

774

775 Figure 4. Calculation of bending moments on segments.

776

777 Figure 5. Sail area and winds in a gust at various heights in the canopy and just above.

778

779 Figure 6. The five felled trees shown as storm-bent. The number of the poorly visible

780 topmost segments that have bent to horizontal ranges from 4 (Tree5) to 11 (Tree2). The

781 green, red and blue horizontal lines represent force vectors caused by wind in the dense

782 simulation on each segment, with the colour indicating whether the drag is caused by the

783 trunk, branches or leaves. The vertical lines represent forces caused by gravity. The length of

784 vertical vectors from the lowest segments is not shown. The bottom end of a vector is -5.7
785 from the lowest segment of Tree5 with the same scale below the 0-level of the Y-axis as
786 above.
787
788 Figure 7. The relative importance of the bending moment caused by gravity acting on
789 segments and associated branches and leaves above the segment in question.
790
791 Figure 8. The dimensions of five felled tree trunks (solid black) and dimensions sufficient to
792 withstand wind and gravity (dotted and dashed lines) in a meteorological situation that
793 causes a mean wind above the canopy of the dense stand (w) of 10.2 m s^{-1}, which is the
794 critical speed that nearly breaks Tree4. The heights on vertical axis and diameters on the
795 horizontal axis are not proportional. Diameters at a height of 1.3 m are given in the bottom.
796 The critical above-canopy wind speed for the dense stand is indicated inside the trunks. The
797 lowest living branches were at heights of 11.2–14.5 m.

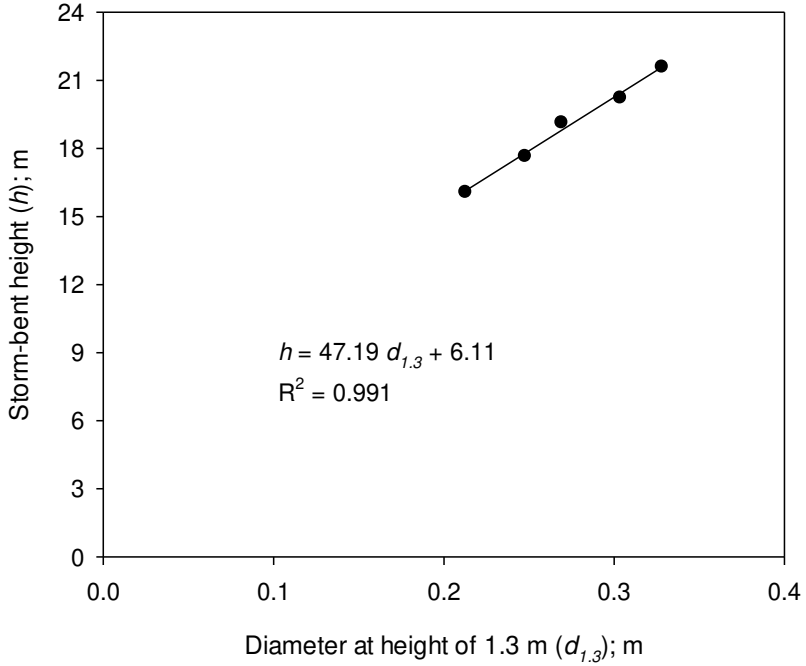

Figure 1. Storm-bent height of the five felled trees plotted against $d_{1.3}$ and a fitted linear regression model. R^2 is the coefficient of determination.

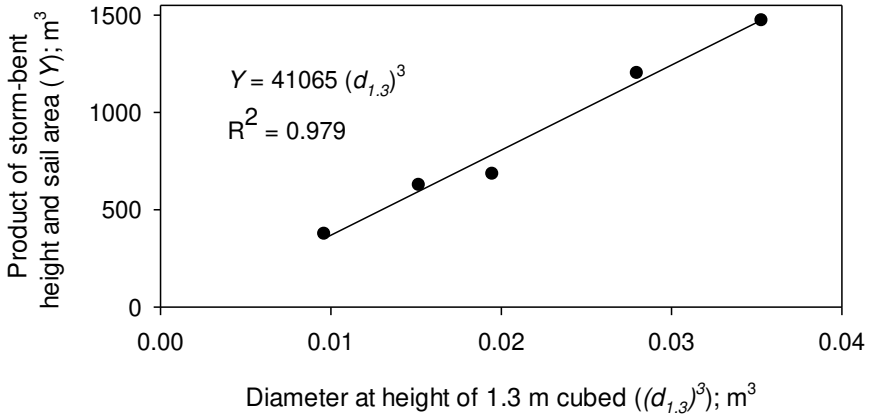

Figure 2. Storm-bent height of the five felled trees multiplied by their sail area (projected area of trunk, branches and leaves) plotted against the cube of $d_{1.3}$ and a fitter linear regression model. R^2 is the coefficient of determination.

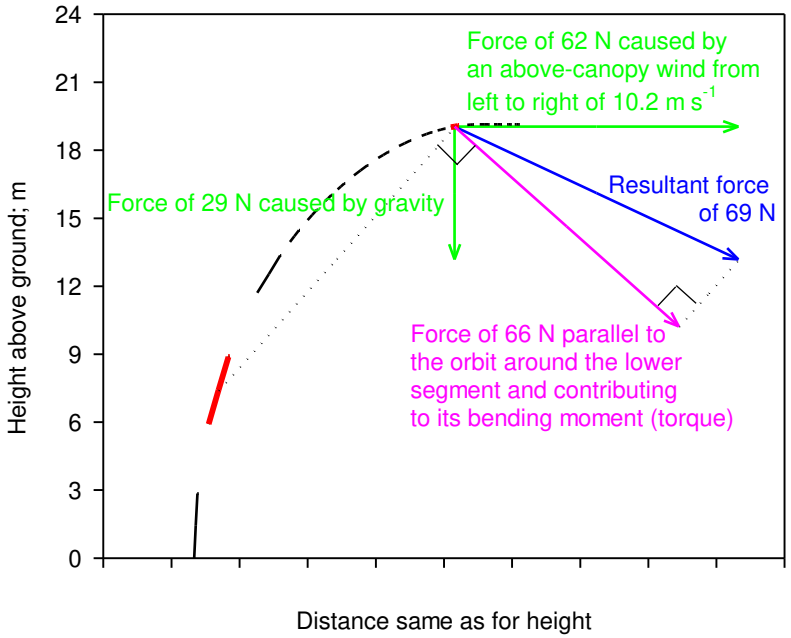

Figure 3. An example of how we computed the bending moments from the forces caused by gravity and wind blowing from left to right. The "dashed" line represents storm-bent Tree3 with 18 uneven segments visible out of its 35 segments. The vectors show how we computed the moment caused by the 11th topmost segment to the 3rd lowest segment (both of which are highlighted with a thicker red line).

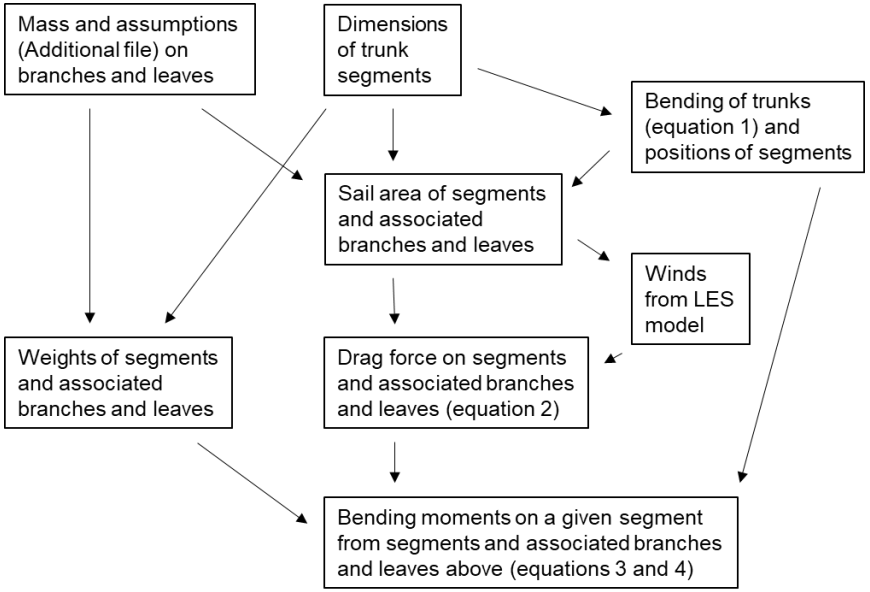

Figure 4. Calculation of bending moments on segments.

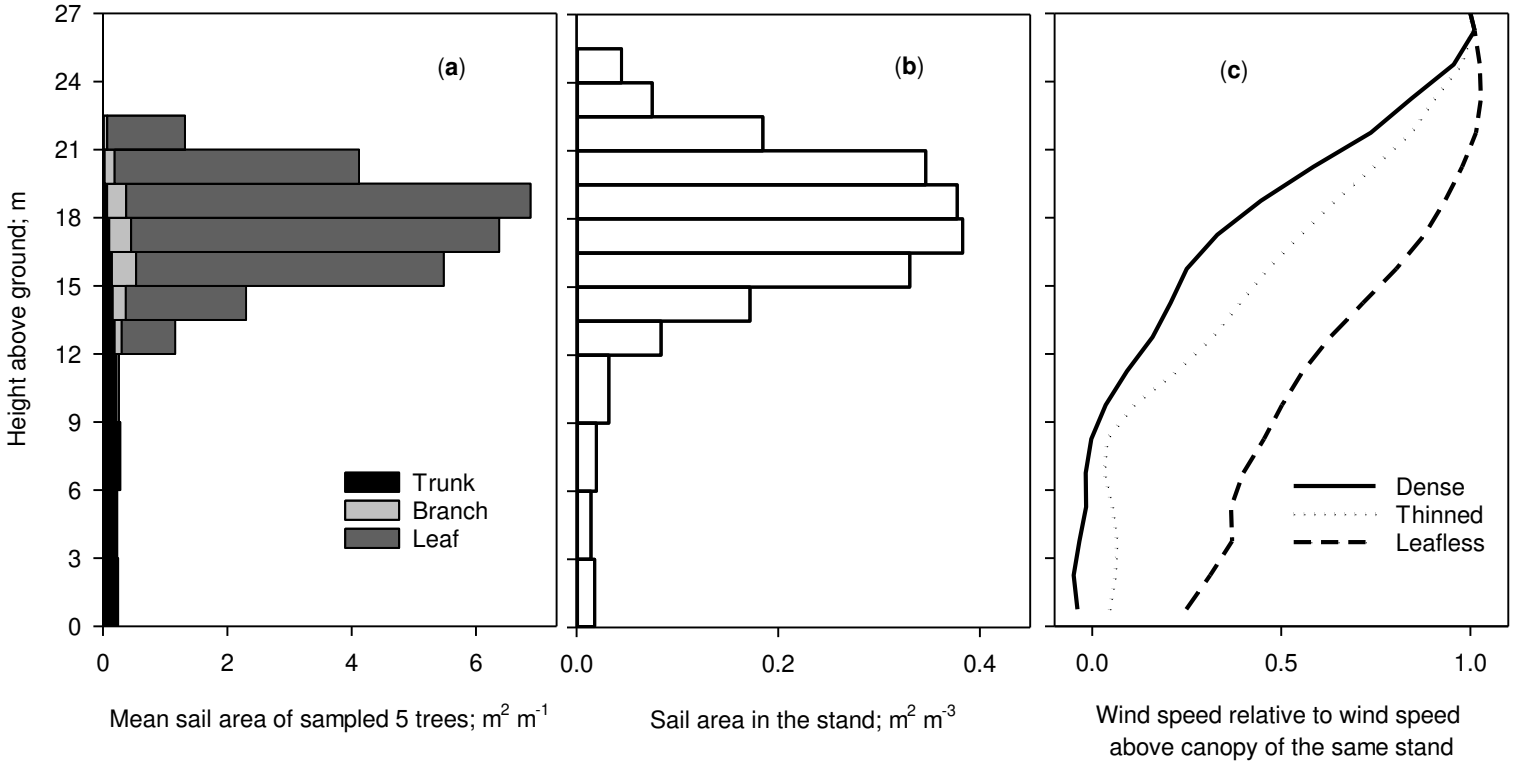

Figure 5. Sail area and winds in a gust at various heights in the canopy and just above.

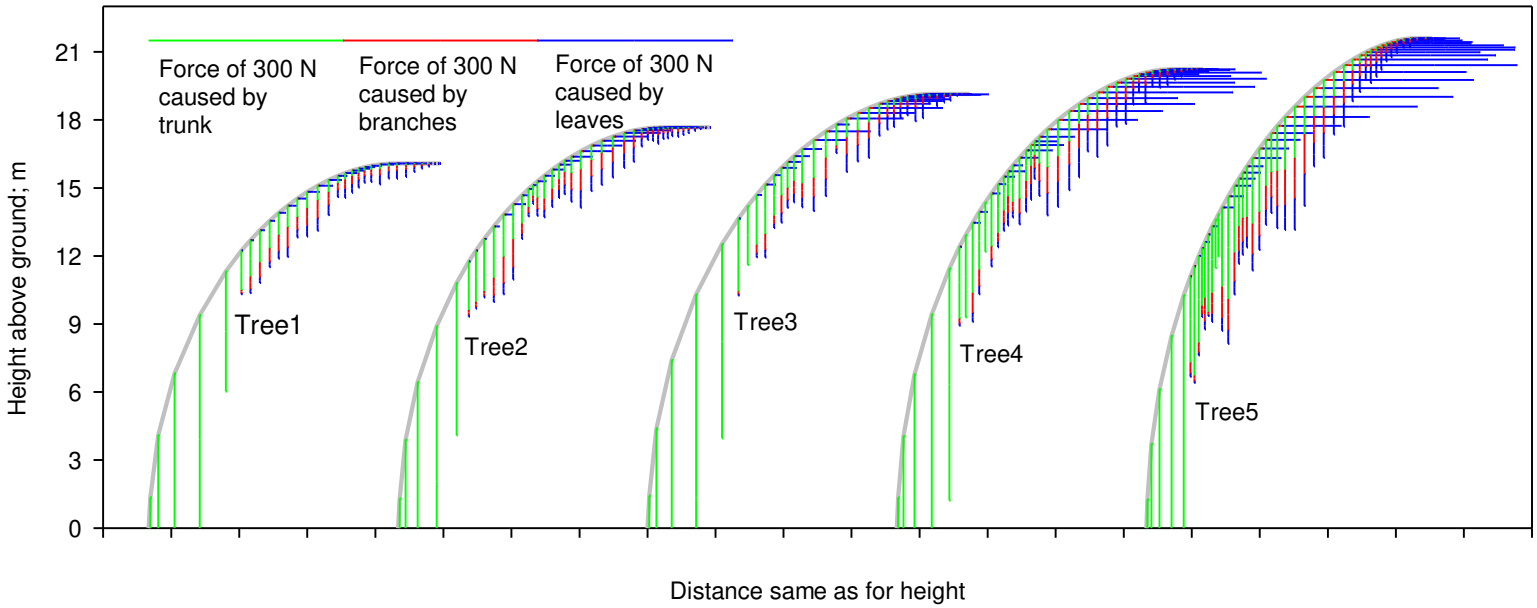

Figure 6. The five felled trees shown as storm-bent. The number of the poorly visible topmost segments that have bent to horizontal ranges from 4 (Tree5) to 11 (Tree2). The green, red and blue horizontal lines represent force vectors caused by wind in the dense simulation on each segment, with the colour indicating whether the drag is caused by the trunk, branches or leaves. The vertical lines represent forces caused by gravity. The length of vertical vectors from the lowest segments is not shown. The bottom end of a vector is -5.7 from the lowest segment of Tree5 with the same scale below the 0-level of the Y-axis as above.

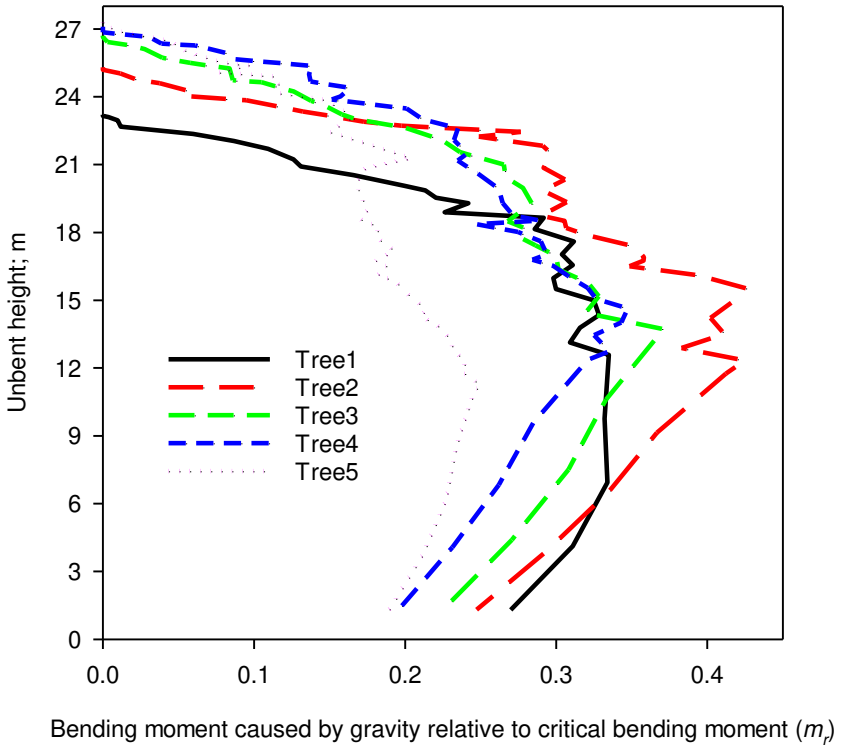

Figure 7. The relative importance of the bending moment caused by gravity acting on segments above the segment in question.

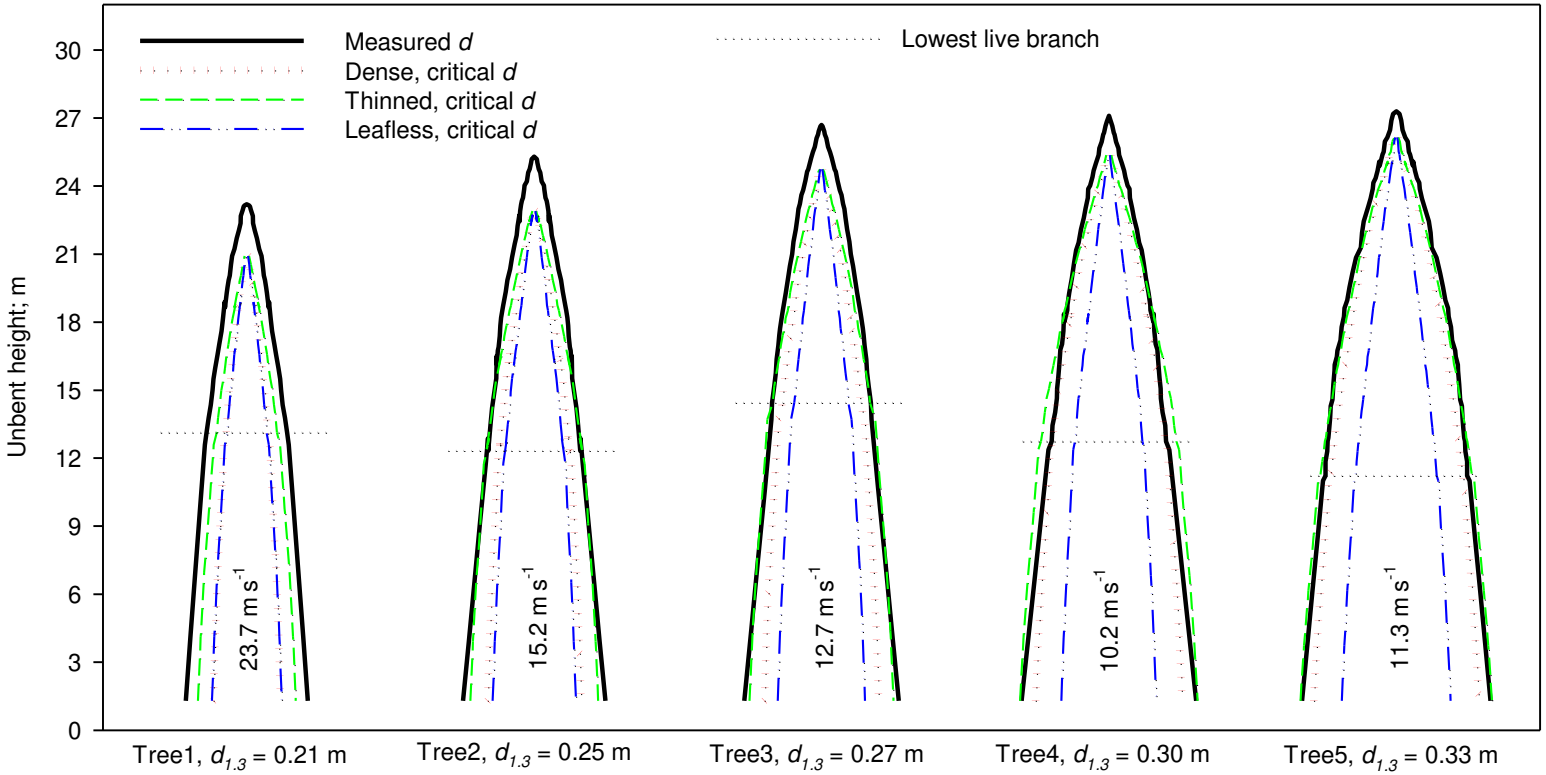

Figure 8. The dimensions of five felled tree trunks (solid black) and dimensions sufficient to withstand wind and gravity (dotted and dashed lines) in a meteorological situation that causes a mean wind above the canopy of the dense stand (w) of 10.2 m s^{-1}, which is the critical speed that nearly breaks Tree4. The heights on vertical axis and diameters on the horizontal axis are not proportional. Diameters at a height of 1.3 m

are given in the bottom. The critical above-canopy wind speed for the dense stand is indicated inside the trunks. The lowest living branches were at heights of 11.2–14.5 m.

Figures

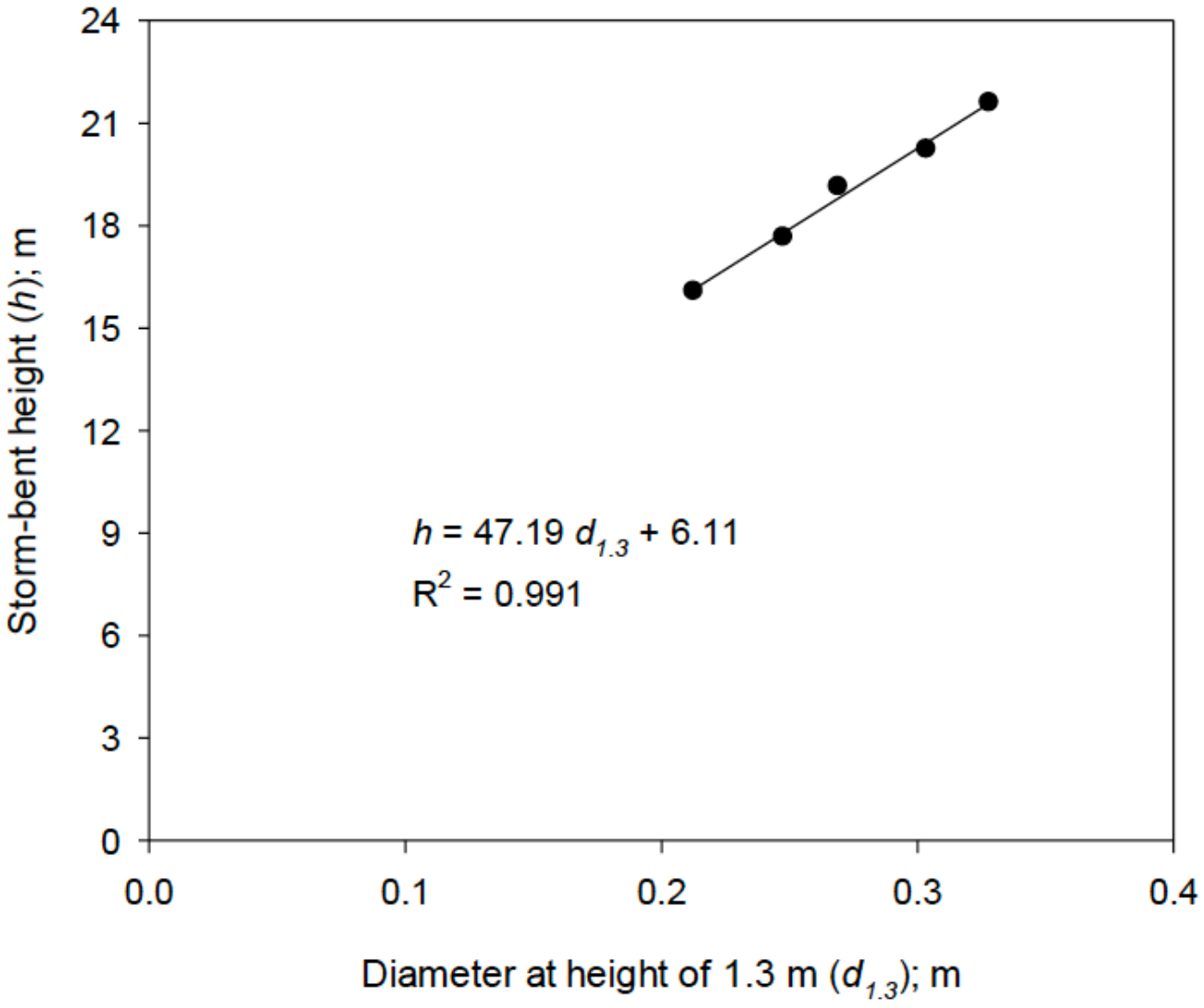

Figure 1

Storm-bent height of the five felled trees plotted against d1.3 and a fitted linear regression model. R2 is the coefficient of determination.

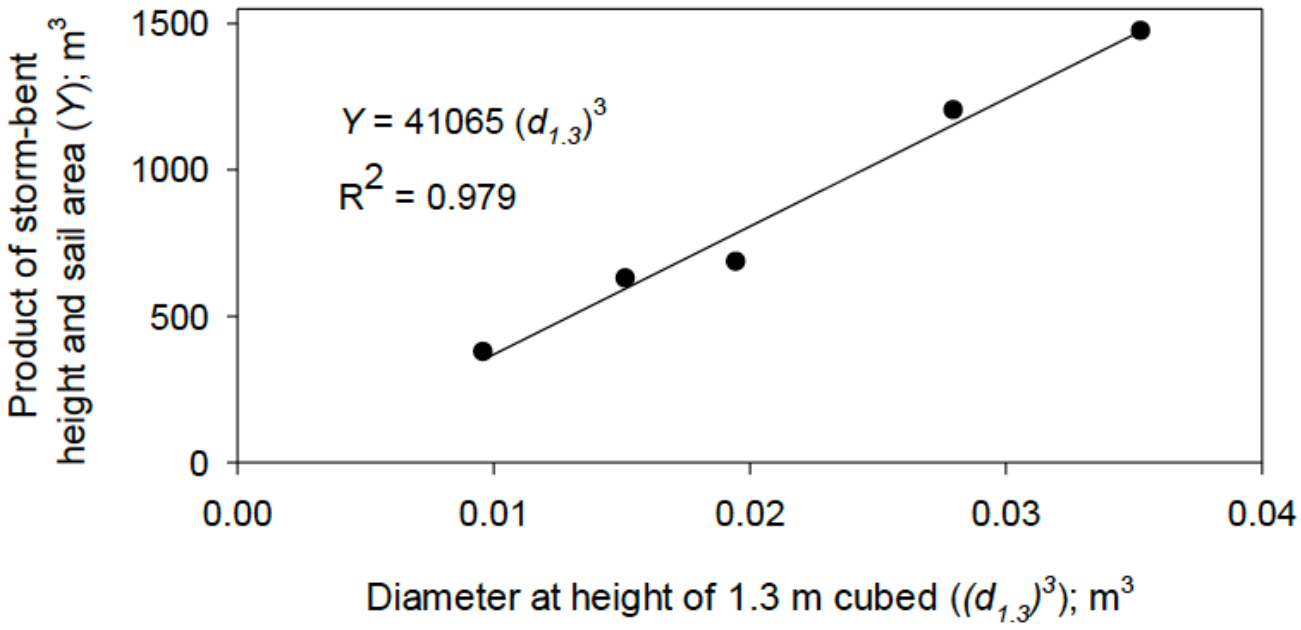

Figure 2

Storm-bent height of the five felled trees multiplied by their sail area (projected area of trunk, branches and leaves) plotted against the cube of d1.3 and a fitter linear regression model. R2 is the coefficient of determination.

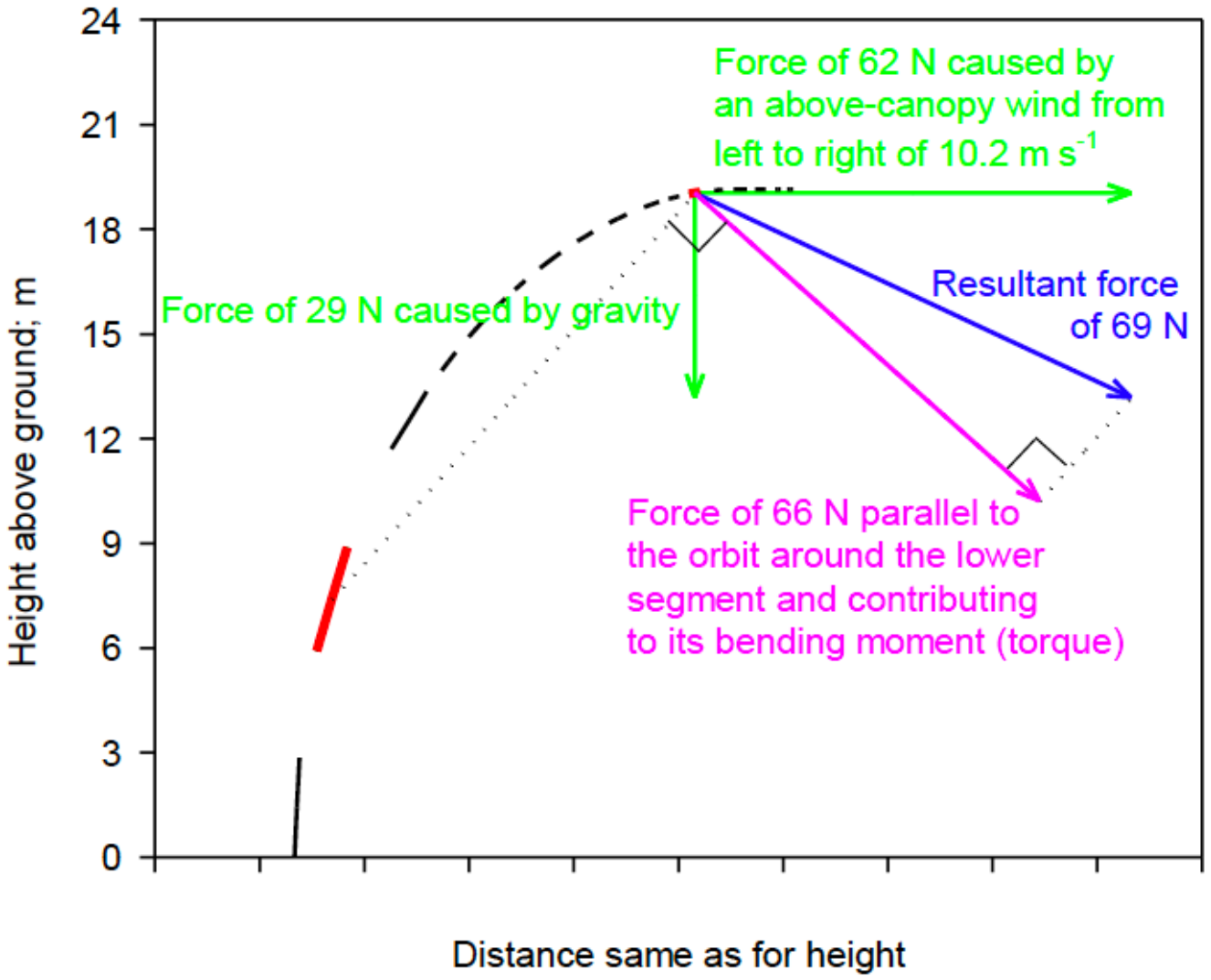

Figure 3

An example of how we computed the bending moments from the forces caused by gravity and wind blowing from left to right. The “dashed” line represents storm-bent Tree3 with 18 uneven segments visible out of its 35 segments. The vectors show how we computed the moment caused by the 11th topmost segment to the 3rd lowest segment (both of which are highlighted with a thicker red line).

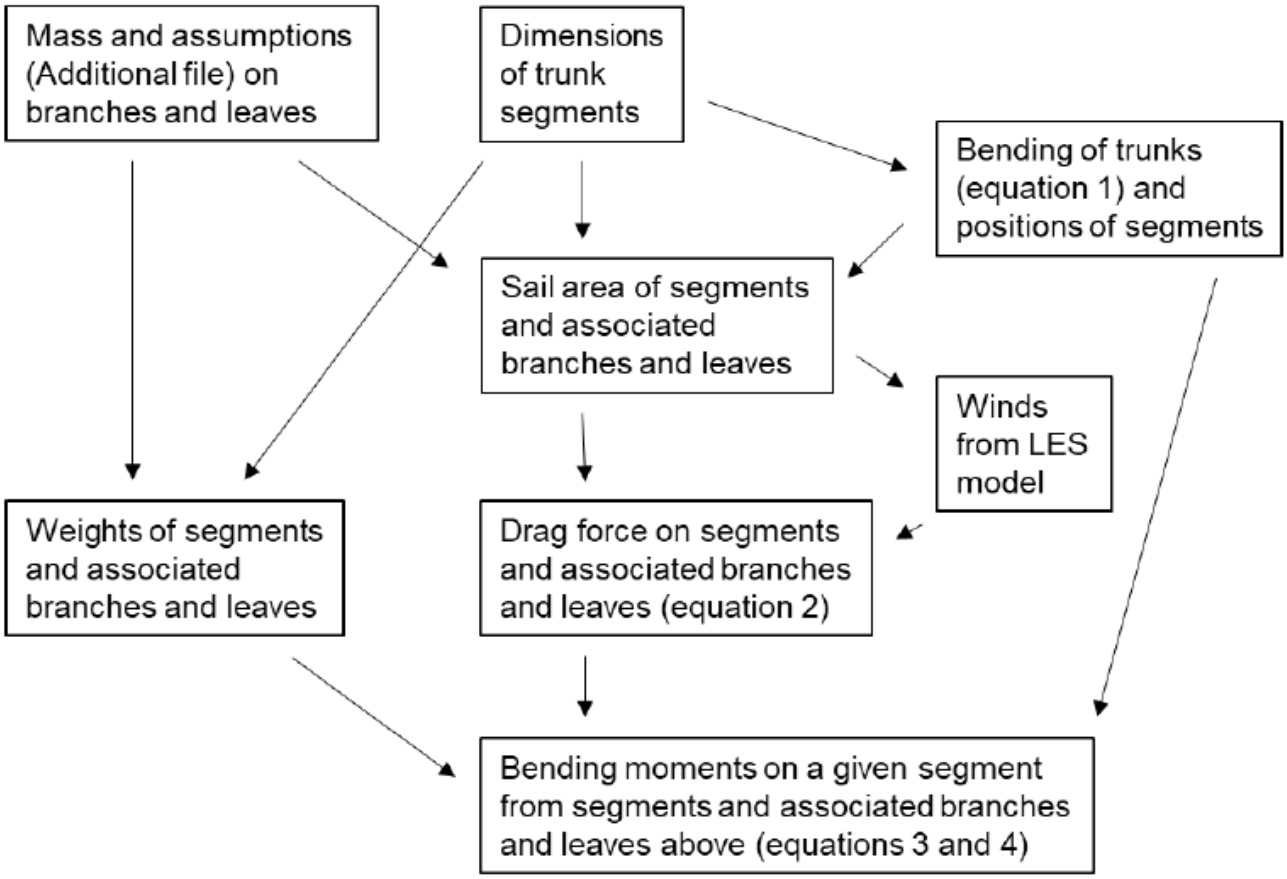

Figure 4

Calculation of bending moments on segments.

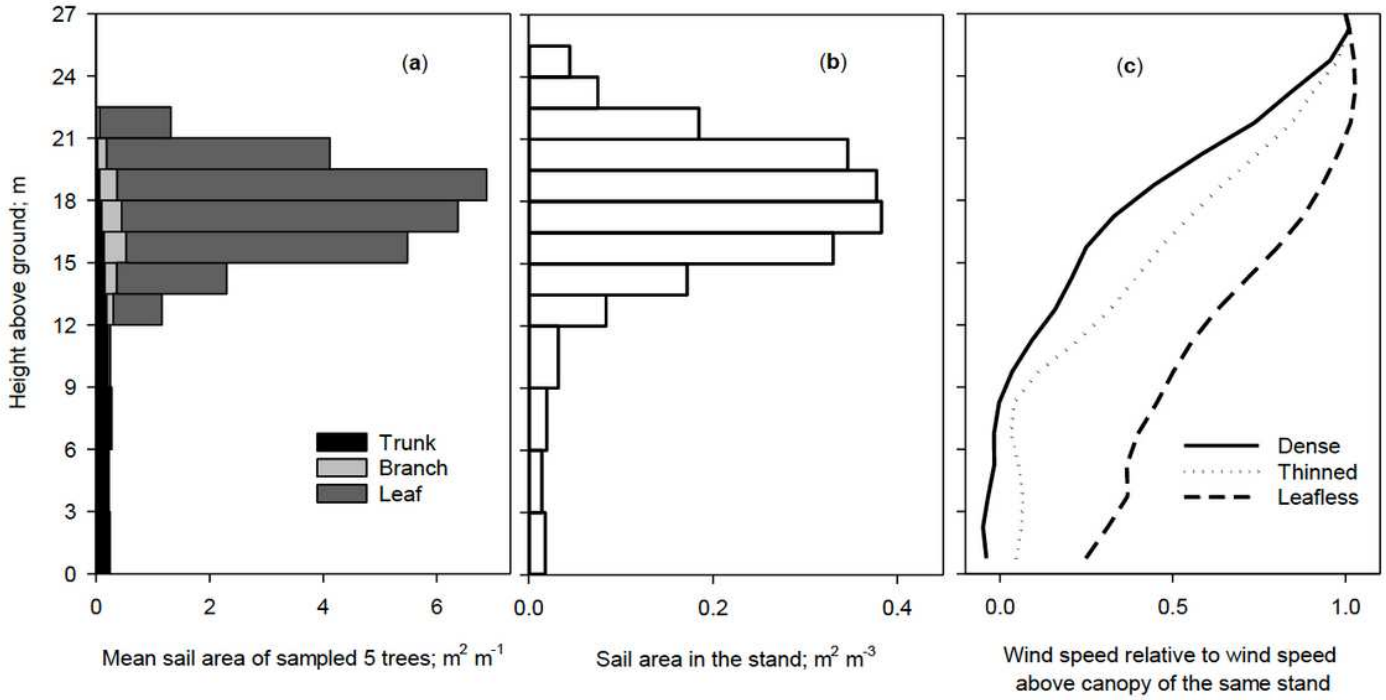

Figure 5

Sail area and winds in a gust at various heights in the canopy and just above.

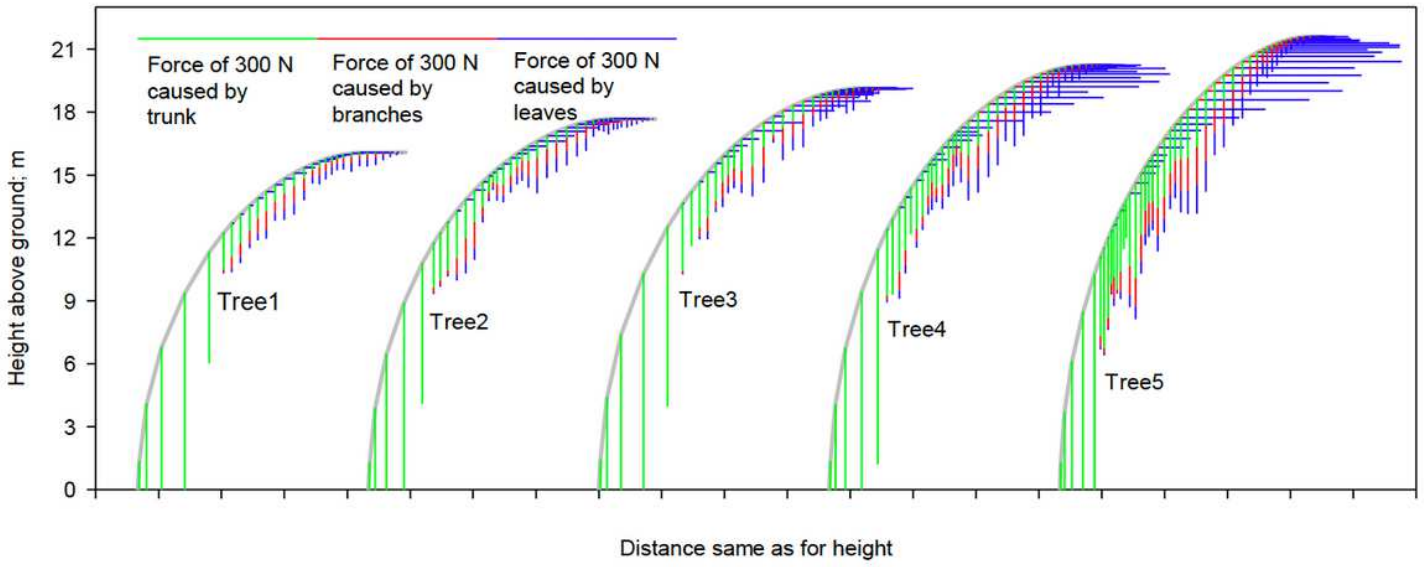

Figure 6

The five felled trees shown as storm-bent. The number of the poorly visible topmost segments that have bent to horizontal ranges from 4 (Tree5) to 11 (Tree2). The green, red and blue horizontal lines represent force vectors caused by wind in the dense simulation on each segment, with the colour indicating

whether the drag is caused by the trunk, branches or leaves. The vertical lines represent forces caused by gravity. The length of vertical vectors from the lowest segments is not shown. The bottom end of a vector is -5.7 from the lowest segment of Tree5 with the same scale below the 0-level of the Y-axis as above.

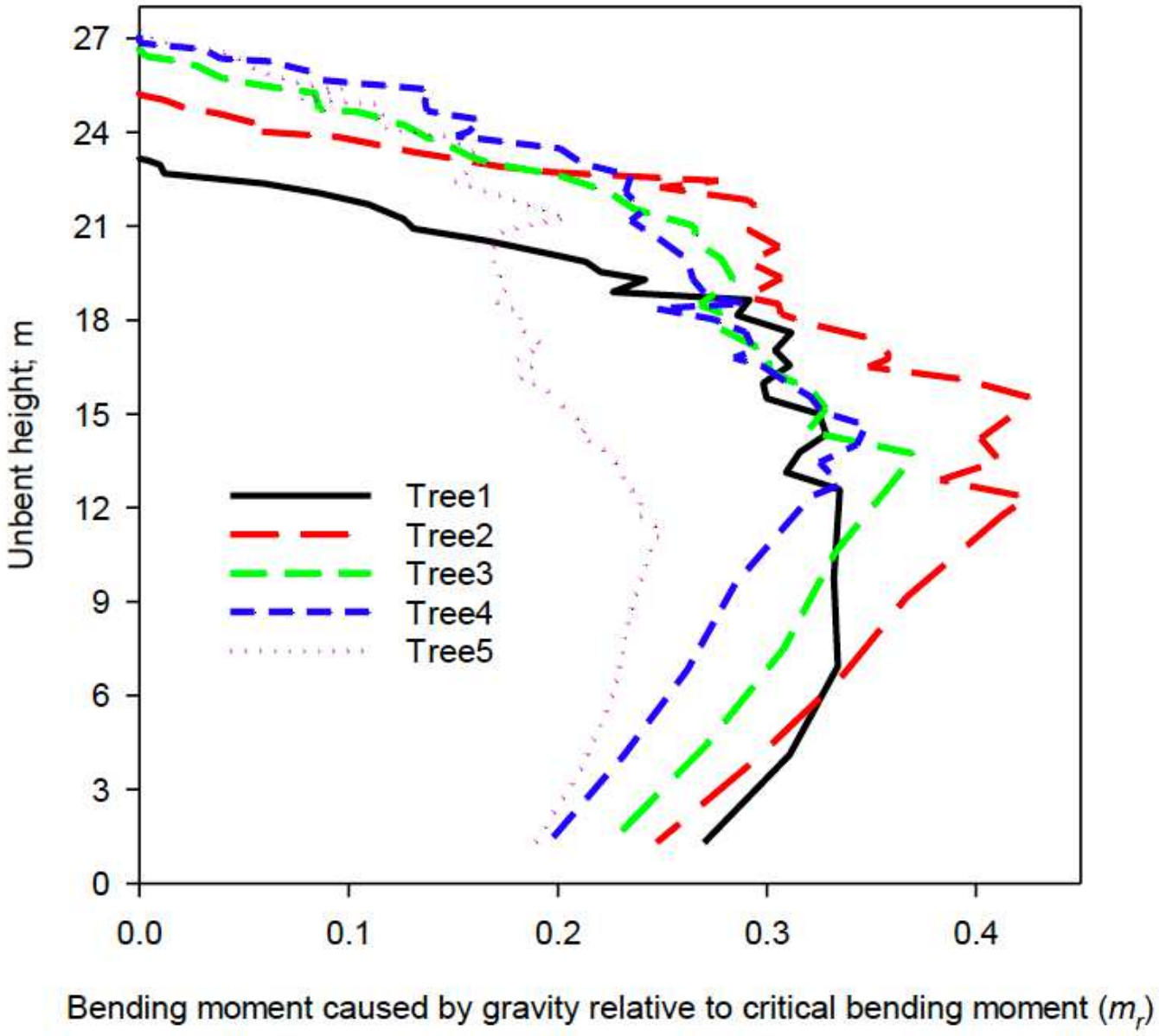

Figure 7

The relative importance of the bending moment caused by gravity acting on segments above the segment in question.

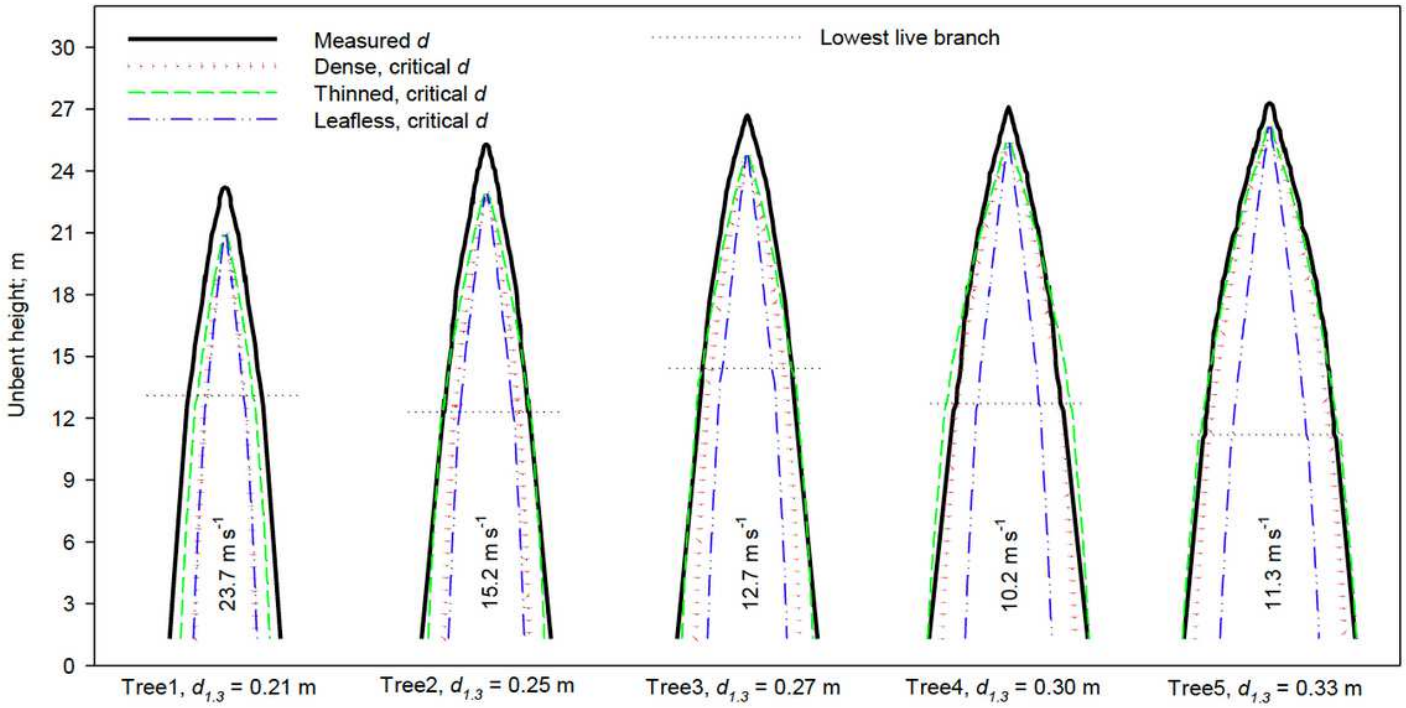

Figure 8

The dimensions of five felled tree trunks (solid black) and dimensions sufficient to withstand wind and gravity (dotted and dashed lines) in a meteorological situation that causes a mean wind above the canopy of the dense stand (w) of 10.2 m s-1, which is the critical speed that nearly breaks Tree4. The heights on vertical axis and diameters on the horizontal axis are not proportional. Diameters at a height of 1.3 m are given in the bottom. The critical above-canopy wind speed for the dense stand is indicated inside the trunks. The lowest living branches were at heights of 11.2–14.5 m.